Hindawi
Geofluids
Volume 2020, Article ID 6610399, 14 pages
https://doi.org/10.1155/2020/6610399

Research Article

Study on Plastic Zone Distribution Characteristic of Coal and Rock Mass in Excavation from Crosscut Coal

Chengwu Li, Xiaoqian Zhang, Chengmin Wei, and Yao Nie

School of Emergency Management and Safety Engineering, China University of Mining and Technology (Beijing), Beijing 100083, China

Correspondence should be addressed to Xiaoqian Zhang; sdslcszxq@163.com

Received 3 December 2020; Revised 8 December 2020; Accepted 11 December 2020; Published 24 December 2020

Academic Editor: Feng Xiong

Coal and gas outburst is a serious disaster in the mining, and crosscut coal is the most prone to cause the coal and gas outburst. In order to study the mechanism of outburst, this paper studied the stress distribution characteristics in front of the working face in the process of rock roadway driving before implementing crosscut coal firstly. On this basis, the hypothesis of stress distribution on the "strong and soft face" of coal-rock mass was proposed. And by using the hypothesis, the mechanical equation for the parameter changes of the plastic zone in front of the working face in crosscut coal was established, and the width and morphological characteristics of the plastic zone in crosscut coal were analyzed. The results show that during the process, as the working face moves forward, the shape distribution of the plastic zone in front of the working face changes from the "semielliptical" to "semibutterfly," And based on the distribution characteristics of plastic zone in working face in crosscut coal, modification proposals for outburst-prevention measures were proposed and provided technical support for the outburst-prevention measures and key parameters setting to prevent the coal outburst in crosscut coal.

1. Introduction

China is rich in coal resources. It is both the world's largest producer and consumer of coal [1]. With the increasing development intensity of coal resource in China, the depth of coal mining is increasing. According to incomplete statistics, the mining depth of China's coal mines is increasing at a rate of 10 to 20 meters per year, and coal mines with depth more than 1000 m are becoming the norm [2, 3]. Deep mine construction and deep mining of mineral resources have become new subjects that coal engineering must face [4]. The deep coal mass is often in a state of high in situ stress and high gas pressure [5], which brings great difficulties and dangers to mine construction and mining. And as the depth of the mine increases, many nonoutburst coal seams have begun to transform into outburst coal seams, and coal and gas outburst have become more and more serious [6, 7]. According to data [8], China has become the country with the most serious coal and gas outburst disasters in the world. The crosscut coal is the most prone to cause the coal and gas outburst [9–11], but its complicated mechanism often causes the failure of conventional prevention and control techniques [12, 13]. Although there are many hypotheses for outburst mechanism, it is possible that these hypotheses can be transformed into effective prediction and prevention methods. Studying the stress transfer and instability process of crosscut coal is helpful to explore effective prediction and technical method of crosscut coal.

In order to reduce the accident of coal and gas outburst in crosscut coal uncovering. In the 1920s, scholars began to study the phenomenon of crosscut coal, and a simple qualitative explanation of it was given. They generally believe that when the roadway approaches the coal seam, the peak of the concentrated stress will appear in the coal seam. At this time, part of the coal mass has been damaged, but due to the protection of the rock mass in front of the coal mass, the coal mass will not lose stability. As the crosscut removed, the high-pressure gas in the coal mass instantly destroyed the damaged coal mass, which caused the outburst of coal and gas. With the continuous in-depth study of the outburst mechanism of crosscut coal, researchers study the outburst as a mechanical phenomenon [14] or a mechanical process [15, 16]. Zhou et al. [17] established a gas-solid coupling

model that comprehensively considered ground stress, gas pressure, and mining depth to study the crosscut coal outburst process and verified the established model through comsol multiphysics simulation software. Wang et al. [18] quantitatively studied the contribution of various factors such as gas pressure, ground stress, and temperature to the gas outburst during coal mining in crosscut coal through laboratory experiments. Black [19] analyzed many typical mine disasters in Australia, and he believed that the comprehensive factors such as gas pressure, coal and rock strength, ground stress, and geological structure were the main factors that caused gas outburst in crosscut coal and proposed effective prediction and technical methods of crosscut coal. Wang et al. [20] analyzed the law between stress distribution, gas pressure, and accidents in mines; they believe that the dynamic disasters in the stope are mainly caused by stress distribution, and the accidents in the roadway are mainly caused by high-pressure gas and pointed out that coal and gas outburst are the result of the combined action of in situ stress and gas energy; either of which will cause the sudden unloading of coal-rock mass to reach the critical failure of coal mass, thus causing coal and gas outburst. Because gas outburst is highly destructive and occurs quickly, it is difficult to conduct field observation of it. Therefore, scholars have conducted laboratory simulation research on it: Yanlu and Quentin [21] believed that coal and gas outburst was caused by gas pressure, moisture content of coal, and gas pressure and proved through experiments that the main energy of outburst is the expansion energy of free gas in coal. Liang et al. [22] believed that the main cause of coal and gas outburst was the rapid desorption of gas, and through self-developed equipment, he studied the amount of gas and carbon dioxide desorption within 1 minute before the outburst occurred.

Numerical simulation methods are a good supplement to experimental research in engineering applications and scientific research. In recent years, many scholars have used numerical simulation to study the mechanism of coal and gas outbursts, and similar simulation experiments have been used to reproduce the phenomenon of coal and gas outbursts. Han and Shi [23] used the software to simulate the changes in underground stress during the process of crosscut coal and analyzed the stress distribution around the roadway. Yu et al. [24] used MATLAB software to analyze the effect of releasing gas expansion energy on outbursts during the process of crosscut coal. Li et al. [25] applied theoretical analysis and numerical simulation to study the relationship between the ground stress and the outburst risk. And the evolution rule of stress and displacement during coal was obtained as the maximum principal stress and crosscut roadway formed different angles. He pointed out that the outburst generally occurs at the coal-rock interface. The stress concentration factor and the displacement variation gradient increase as the angle between the crosscut and the maximum principal stress increases. Therefore, the drifting direction of the crosscut coal should be as parallel as possible to the maximum principal stress. Griffith et al. [26] studied the disturbance and influence rule of ground stress during the crosscut coal through numerical calculation and actual monitoring and calculated the disturbance stress by applying boundary element to obtain the specific moment when the compressive stress surges as the coal mass deforms and breaks. Jiang et al. [27, 28] applied acoustic emission technology and detection system to conduct predictive experiments of coal and gas outburst. Gao et al. [29] used COMSOL Multiphysics software to analyze the role of underground stress in the process of crosscut coal. Tang and Liu [30] used the PFPA2D system to numerically simulate outbursts in steep coal seams during the process of crosscut coal and analyzed the effects of underground stress and gas pressure on inducing outbursts.

Although scholars have conducted extensive research on the outbursts in crosscut coal and have achieved fruitful results, as a dynamic process from rock roadway to coal roadway, scholars has never reached a consensus on the mechanism of outbursts in crosscut coal due to the differences in the physico-mechanical properties of coal-rock mass and the complexity of the mining environment. Moreover, researchers usually take the method of using borehole to discharge stress as the main outburst-prevention measure in crosscut coal. However, due to the lack of characteristic parameters of the stress distribution area in front of the working face, the researchers can only assume that the stress distribution in front of the working face is uniform. Therefore, detailed rules for the Prevention and Control of Coal and Gas outburst also require the uniform arrangement of drainage borehole, which wastes a lot of engineering costs and affects the speed of roadway driving. Understanding the distribution characteristics of the plastic deformation zone in the coal mass in front of the working face is helpful to avoid danger zones during borehole construction, and arranging the boreholes in the elastic deformation zone can have a better stress discharge effect.

In this paper, the stress distribution characteristics in front of the working face during rock roadway excavation before implementing crosscut coal are studied, and a mechanical model of the stress distribution of coal-rock mass and plastic zone width characteristics in front of the semicircle arch roadway in the polar coordinates under nonuniform conditions is constructed; the hypothesis of stress distribution on the "strong and soft face" of coal-rock mass in crosscut coal is proposed, and combined with the mechanical model, the stress state calculation model when the crosscut breaks through the coal seam is established, and the fact that the shape of the plastic zone changes from "semidumbbell" to "semibutterfly" is confirmed. Finally, to verify the correctness of the theory of crosscut coal, this article uses Flac3D software to simulate the overall process of crosscut coal.

2. Study on Distribution Characteristics of Plastic Zone of Coal-Rock Mass in Driving Face

Before the excavations begin, the coal-rock mass under triaxial compression is in a state of stress balance, and roadway excavation breaks this original natural stress state. Subsequently, in the form of energy, part of the in situ stress is transferred to the deep part of the surrounding rock, and part is released with the driving operation, resulting in a redistribution of the stress. As a result, the tangential stress increases and the radial stress decreases; the stress in front of the

driving face reaches its extreme value, and the stress concentration in a local area appears. Specifically, the stress state in front of the working face shows that the coal-rock mass has been in cyclic loading-unloading process as "mining and unloading—stress shift —stress concentration," etc. The roadway excavation will cause the redistribution of the stress in coal mass in front of the working face. Therefore, according to the degree of deformation and destruction of the coal mass, it can be divided into the plastic zone, the stress concentration zone, and the elastic zone (as shown in Figure 1).

2.1. Mechanical Model of Stress State of Driving Face. Assuming that the surrounding rock of the drift is not effected by factors such as geological structure, water, and rock structure, the in situ stress field is only composed of the self-weight stress field, and using the two-dimensional stress distribution solution around the circular hole in the elastic plate of the elastic mechanics, the stress expression in the elastic zone in front of the spherical driving face under polar coordinates can be obtained: expressed as the radial stress at any point [31]:

$$\begin{cases} \sigma_r = \dfrac{1}{2}P_0(1+\lambda)\left(1-\dfrac{R_0^2}{r^2}\right)-\dfrac{1}{2}\mathrm{P}_0(1-\lambda)\left(1-4\dfrac{R_0^2}{r^2}+3\dfrac{R_0^4}{r^4}\right)\cos 2\theta, \\ \sigma_\theta = \dfrac{1}{2}P_0(1+\lambda)\left(1+\dfrac{\mathrm{R}_0^2}{\mathrm{r}^2}\right)+\dfrac{1}{2}\mathrm{P}_0(1-\lambda)\left(1+3\dfrac{r_\mathrm{p}^4}{r^4}\right)\cos 2\theta, \\ \tau_{r\theta} = \dfrac{1}{2}P_0(1-\lambda)\left(1+2\dfrac{R_0^2}{r^2}-3\dfrac{R_0^4}{r^4}\right)\sin 2\theta, \\ \sigma_\mathrm{z} = \mu(\sigma_r+\sigma_\theta). \end{cases} \tag{1}$$

In this expression, σ_r expressed as the radial stress at any point; σ_θ expressed as the hoop stress at any point; $\tau_{r\theta}$ expressed as the shear stress at any point σ_z expressed as the stress in the z direction at any point; P_0 expressed as the overburden pressure; λexpressed as the coefficient of lateral pressure; R_0 expressed as the radius of the driving face; r, θ expressed as the polar coordinates of any point.

Along the drift direction, as the distance to the working face increases, the stress in the coal-rock mass increases gradually as well, if the pressure of the coal-rock mass beyond the strength limit, the destruction will develop deeper into the coal mass until the compressive strength of the coal mass is equal to the peak stress. Therefore, the stress in the plastic zone is the ultimate stress that the fractured rock mass can bear, which mainly determined by the limit equilibrium condition of the rock mass. According to the limit equilibrium condition of the rock mass, the stress expression in the plastic zone can be obtained:

$$\begin{cases} \sigma_{rp} = \mathrm{Kctg}\varphi\left[\left(\dfrac{r}{R_0}\right)^{2\sin\varphi/(1-\sin\varphi)}-1\right], \\ \sigma_{\theta p} = \mathrm{Kctg}\varphi\left[\dfrac{1+\sin\varphi}{1-\sin\varphi}\left(\dfrac{r}{R_0}\right)^{2\sin\varphi/(1-\sin\varphi)}-1\right], \\ \tau_{r\theta p} = 0. \end{cases} \tag{2}$$

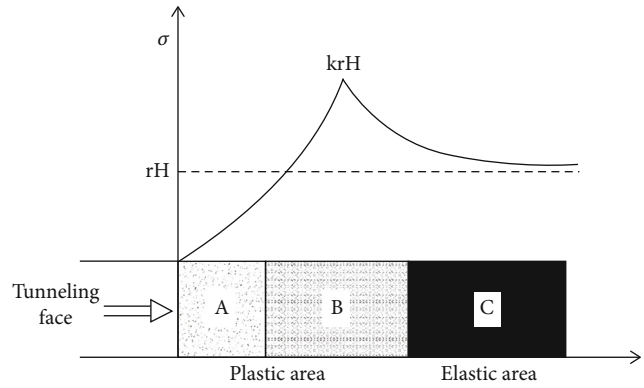

Figure 1: Schematic diagram of regional distribution of mining stress field.

In this expression: σ_{rp} expressed as the radial stress at any point in the plastic zone; $\sigma_{\theta p}$ expressed as the hoop stress at any point in the plastic zone; K expressed as the cohesion of coal rock mass; φ expressed as the internal friction angle of the coal-rock mass.

If the coal-rock mass at the elastic-plastic interface meets both the stress conditions in the elastic zone and the plastic zone, assuming that R_p expressed as the radius of the plastic zone, according to the stress continuity condition and the boundary condition:

$$\begin{cases} r = R_p, \sigma_{rp} = \sigma_\mathrm{r}, \sigma_{\theta p} = \sigma_\theta, \tau_{r\theta p} = \tau_{r\theta} = 0, \\ (\sigma_r)_{r>>R_0} = -P' \cos 2\theta \ (\tau_{r\theta})_{r>>R_0} = -P' \sin 2\theta. \end{cases} \tag{3}$$

The expressions of stress and radius of the plastic zone in front of the driving face can, respectively, be obtained:

$$\begin{cases} \sigma_r = \dfrac{1}{2}P_0(1+\lambda)-\dfrac{r_p^2\sin\varphi}{2r^2}[P_0(1+\lambda)+2K\mathrm{ctg}\varphi]-\dfrac{1}{2}P_0(1-\lambda)\left(1-4\dfrac{r_p^2}{r^2}+3\dfrac{r_p^4}{r^4}\right)\cos 2\theta, \\ \sigma_\theta = \dfrac{1}{2}P_0(1+\lambda)+\dfrac{r_p^2\sin\varphi}{2r^2}[P_0(1+\lambda)+2K\mathrm{ctg}\varphi]+\dfrac{1}{2}P_0(1-\lambda)\left(1+3\dfrac{r_p^4}{r^4}\right)\cos 2\theta, \\ \tau_{r\theta} = \dfrac{1}{2}P_0(1-\lambda)\left(1+2\dfrac{r_p^2}{r^2}-3\dfrac{r_p^4}{r^4}\right)\sin 2\theta, \end{cases} \tag{4}$$

$$\begin{cases} \sigma_{rp} = \mathrm{Kctg}\varphi\left[\left(\dfrac{r}{R_0}\right)^{2\sin\varphi/(1-\sin\varphi)}-1\right], \\ \sigma_{\theta p} = \mathrm{Kctg}\varphi\left[\dfrac{1+\sin\varphi}{1-\sin\varphi}\left(\dfrac{r}{R_0}\right)^{2\sin\varphi/(1-\sin\varphi)}-1\right], \end{cases} \tag{5}$$

$$R_p = R_0\left\{\frac{[P_0(1+\lambda)+2K\mathrm{ctg}\varphi](1-\sin\varphi)}{2K\mathrm{ctg}\varphi}\right\}^{(1-\sin\varphi)/2\sin\varphi} \cdot\left\{1+\frac{(1-\sin\varphi)P_0(1+\lambda)\cos 2\theta}{\sin\varphi[P_0(1+\lambda)+2K\mathrm{ctg}\varphi]}\right\}. \tag{6}$$

In this expression,

$$r_p = R_0 \left\{ \frac{[P_0(1+\lambda) + 2K\mathrm{ctg}\varphi](1-\sin\varphi)}{2K\mathrm{ctg}\varphi} \right\}^{(1-\sin\varphi)/2\sin\varphi}. \tag{7}$$

Equations (4), (5), and (6) are analytical solutions for the stress distribution in front of the driving face and the width of the plastic zone.

2.2. Stress Distribution and Plastic Zone Distribution Characteristics in Front of Driving Face. Assuming that the overburden pressure is 20 MPa (equivalent to a mine depth of 800 meters), coefficient of lateral pressure is 0.5, and the radius of the drift is 2 m. According to the table of rock mechanics parameters, the internal friction angle of the coal mass is 20°, and the cohesion is 2 MPa; the internal friction angle of the mudstone is 25°, and the cohesion is 3 MPa; the internal friction angle of the shale is 30°, and the cohesion is 4 MPa. According to the stress calculation expressions of (4) and (5), the hoop stress distribution in front of the driving face under different coal-rock mass is shown in Figure 2.

In Figure 2(a), the abscissa indicates the driving direction, the ordinate on the left indicates the size of the drift, and the ordinate on the right indicates the stress value in front of the driving face. The black curve indicates the hoop stress field distribution in front of the working face of the coal drift, the red curve indicates the circumferential stress field distribution in front of the working face of the mudstone drift, and the blue curve indicates the hoop stress field distribution in front of the working face of the shale drift.

It can be seen from Figure 2(a) that stress concentration occurs in front of the working face. The plastic zone is on the left side of the stress concentration peak, and the elastic zone is on the right. Among them, shale has the highest intensity, strong hardness, the most obvious concentrated stress effect, the highest peak stress, and the fastest hoop stress increment in front of the working face. The coal mass is smaller in intensity than rock, and it is more stable. Under the effect of the same mining activities, the destruction zone has the widest range. In the figure, the concentrated stress peak of the coal mass is the smallest, the range of the plastic zone is the largest, and the range of the elastic zone is the smallest. Therefore, different lithologies have a significant effect on the stress distribution of the driving face.

Figure 2(b) shows the distribution shape and size of the plastic zone in front of the working face for different rocks. Red indicates coal mass, blue indicates mudstone, and purple indicates shale. It can be seen from the figure that as conditions such as mine depth, coefficient of lateral pressure, and size of the drift remain unchanged, the distribution and width of the plastic zone in front of the drift working face with various lithology are different. According to the distribution shape of the plastic zone, the distribution of plastic zone in front of the rock roadway is "semidumbbell" before implementing crosscut coal, and the shale form changes minimally; according to the width of the plastic zone, the width of the plastic zone in front of the coal working face of coal drift is the largest, and the width of the plastic zone in the driving direction is 4 times that of the shale drift.

3. Study on Distribution Characteristics of Plastic Zone of Coal-Rock Mass in Roadway of Crosscut Coal

Crosscut coal means that the driving face starts from the minimum normal distance of 5 m from the bottom (top) plate of the coal seam and ends at 2 m through the coal seam into the top (bottom) plate. Assuming that the driving face is hemispherical, the surrounding rock is homogeneous, isotropic, of linear elasticity, and of no creep properties or sticky behavior.

3.1. The Hypothesis of "Strong and Soft Face" of Stress Distribution on Working Face. The process of crosscut coal is from the rock mass to the coal mass. To study this process, we analyze the rock-coal-rock mass perpendicular to the coal seam as a whole; its mechanical properties (elastic modulus, Poisson's ratio, cohesion, internal friction angle, etc.) are determined by the coal mass and the rock mass; the intensity of the rock mass is greater than that of the coal-rock mass and greater than that of the coal mass [32].

Assuming the driving direction is the x, the direction perpendicular to the coal mass is the x', β is the angle between the polar coordinate radial direction and the direction perpendicular to the coal seam. As shown in Figure 3, define the forward direction of x' as the soft face, and the reverse direction of x' as the strong face.

That is, the soft face is parallel to the front of the coal seam, and the strong face is in the opposite direction. σ_r expressed as the radial stress at any point; σ_θ expressed as the hoop stress at any point; if the inclination of the coal seam is 20 degrees, along the direction of x, the polar angle of driving direction from -20 degrees to 90 degrees is the soft face, and -90 degrees to -20 degrees is the strong face. Because the strong face only exists in rock mass, the stress and distribution of plastic zone are calculated according to the properties of rock mass, and the soft face is calculated based on the mechanical properties of coal-rock mass.

In the process of crosscut coal, assuming the cohesion and internal friction angle of the coal-rock mass in the x' direction are k_1 and φ_1, and the cohesion and internal friction angle in the y' direction are k_2 and φ_2.

The coordinate between the stress at any point in front of the driving face $(\sigma_r, \sigma_\theta, \tau_{r\theta})$ and $(\sigma_{x'}, \sigma_{y'}, \tau_{x'y'})$ is converted to

$$\begin{cases} \sigma_r = \sigma_{x'}\cos^2\beta + \sigma_{y'}\sin^2\beta - 2\tau_{x'y'}\sin\beta\cos\beta, \\ \sigma_\theta = \sigma_{x'}\sin^2\beta + \sigma_{y'}\cos^2\beta + 2\tau_{x'y'}\sin\beta\cos\beta. \end{cases} \tag{8}$$

According to theory of the Mohr's Circle,

$$\tau_{x'y'} = \frac{\sigma_r - \sigma_\theta}{2}\sin\beta. \tag{9}$$

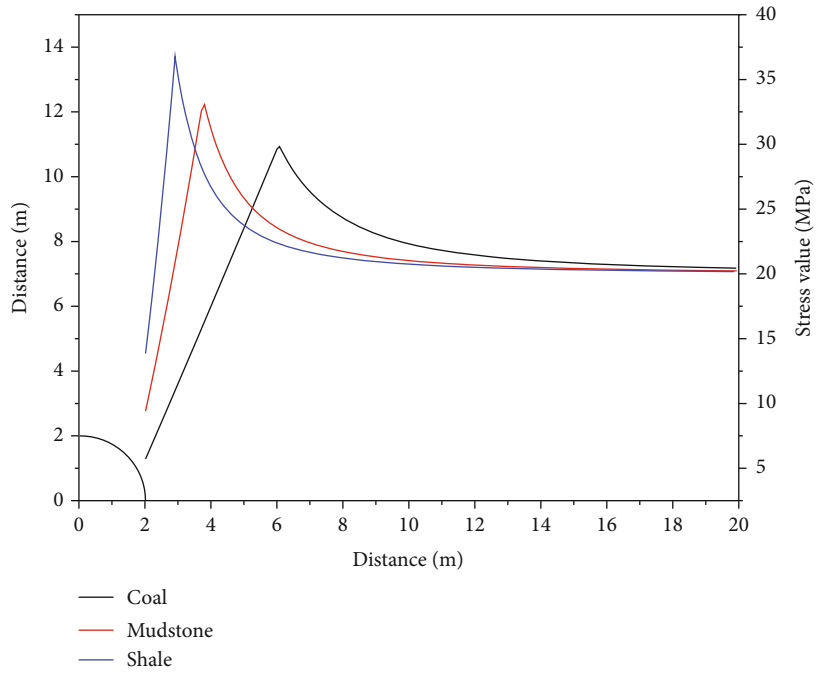

(a) The effect of lithology on stress distribution

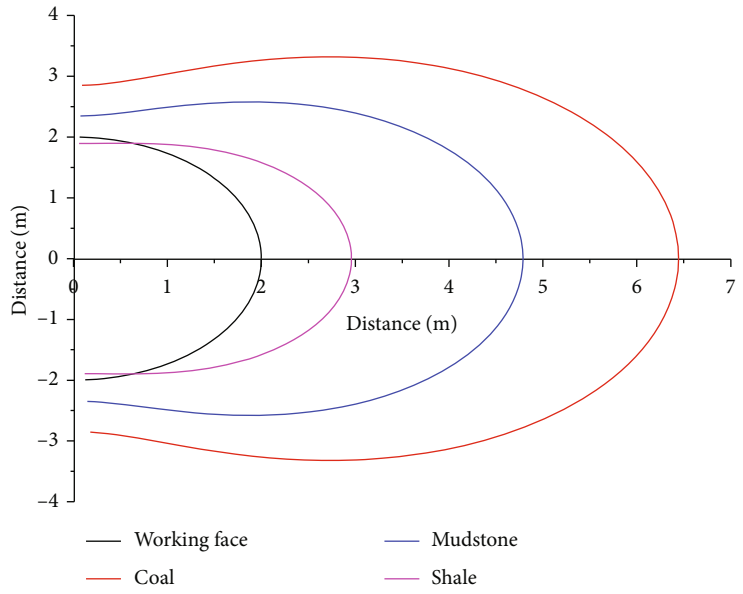

(b) The effect of lithology on the width of the plastic zone

Figure 2: Relationship between lithology and original rocks.

Unite Equation (8) and Equation (9):

$$\begin{cases} \sigma_r = \sigma_{x'} \cos^2\beta + \sigma_{y'} \sin^2\beta - \dfrac{\left(\sigma_{x'}\left(\cos^2\beta\text{-}\sin^2\beta\right) + \sigma_{y'}\left(\sin^2\beta - \cos^2\beta\right)\right) \sin^2 2\beta}{2\left(1 + \sin^2 2\beta\right)}, \\ \sigma_\theta = \sigma_{x'} \sin^2\beta + \sigma_{y'} \cos^2\beta + \dfrac{\left(\sigma_{x'}\left(\cos^2\beta\text{-}\sin^2\beta\right) + \sigma_{y'}\left(\sin^2\beta - \cos^2\beta\right)\right) \sin^2 2\beta}{2\left(1 + \sin^2 2\beta\right)}. \end{cases} \tag{10}$$

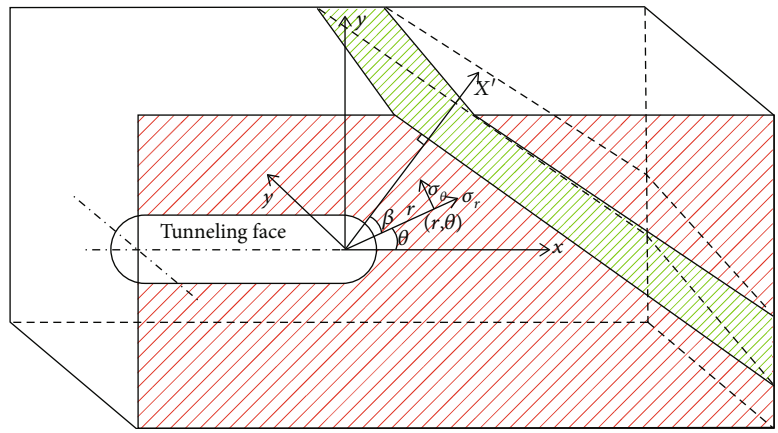

Figure 3: Hypothesis of the "strong and soft face" in crosscut coal.

According to Mohr's strength theory,

$$\sigma_1 = \frac{1+\sin\varphi}{1\text{-}\sin\varphi}\sigma_3 + \frac{2k\cos\varphi}{1\text{-}\sin\varphi}. \tag{11}$$

Assuming that $a_1 = 2k\cos\varphi/(1-\sin\varphi)$, then $\sigma_1 = (1+\sin\varphi)/(1-\sin\varphi)\sigma_3 + a_1$; if $\sigma_3 = 0$, $\sigma_1 = a_1$. Since the stress satisfies the coordinate transformation, a_1 satisfies the coordinate transformation as well.

In the x' direction, a_1 means $a_{x'} = 2k_1\cos\varphi_1/(1-\sin\varphi_1)$. In the y' direction, a_1 means $a_{y'} = 2k_2\cos\varphi_2/(1-\sin\varphi_2)$. According to Equation (10), the radial expression and the hoop expression of any point a_1 are obtained:

$$\begin{cases} a_r = a_{x'}\cos^2\beta + a_{y'}\sin^2\beta - \dfrac{\left(a_{x'}\left(\cos^2\beta\text{-}\sin^2\beta\right) + a_{y'}\left(\sin^2\beta-\cos^2\beta\right)\right)\sin^2 2\beta}{2\left(1+\sin^2 2\beta\right)}, \\ a_\theta = a_{x'}\sin^2\beta + a_{y'}\cos^2\beta + \dfrac{\left(a_{x'}\left(\cos^2\beta\text{-}\sin^2\beta\right) + a_{y'}\left(\sin^2\beta-\cos^2\beta\right)\right)\sin^2 2\beta}{2\left(1+\sin^2 2\beta\right)}. \end{cases} \tag{12}$$

In this expression,

$a_x{}'$ is determined by coal-rock mass k_1, φ_1. For $a_y{}'$, if the plastic zone exists in rock mass, it is determined by the parameters of the rock mass, $a_{y'} = 2k_{y'}\cos\varphi_y/(1-\sin\varphi_y)$ (k_y refers to cohesion of the rock mass; φ_y refers to internal friction angle of the rock mass). If the plastic zone exist in coal mass, $a_{y'} = 2k_m\cos\varphi_m/(1\text{-}\sin\varphi_m)$ (k_m refer to cohesion of the coal mass; φ_m refers to internal friction of coal mass).

As the driving face advances, the thickness of the rock mass decreases gradually, and the parameters of coal-rock mass (k_1, φ_1) decrease as well, getting closer to the coal seam parameters little by little. Assume that k_1 and φ_1 decrease linearly with the change of thickness h_1 (h_1 refers to the vertical distance between the working face and the coal seam) (as shown in Figure 4).

When h_1 is much greater than the h_2 (the thickness of coal mass), the mechanical properties of the soft face direction are basically equal to the mechanical properties of the rock mass. When h_1 is the smaller one, they are close to that of coal mass. Therefore, this paper designs a threshold h_b, when $h_b \le h_1$, the mechanical properties of the soft face direction are determined by the mechanical properties of the rock mass; when $h_b \ge h_1$, they are determined by that of coal-rock mass. During the crosscut coal, $h_1 = 0$, then the mechanical parameters of the soft face direction are equal to the mechanical parameters of the coal mass. For different coal mines, the properties of rock mass and coal mass in front of the driving face are different, the mechanical properties of the coal-rock mass determined by it are different as well. For any specific coal mine, the mechanical parameters of the coal-rock mass should be experimentally determined and then substituted into the formula to solve.

From Figure 4, we can see

$$\begin{cases} K_1 = k_m + \dfrac{h_1}{h_b}\left(k_y\text{-}k_m\right), \\ \varphi_1 = \varphi_m + \dfrac{h_1}{h_b}\left(\varphi_y\text{-}\varphi_m\right). \end{cases} \tag{13}$$

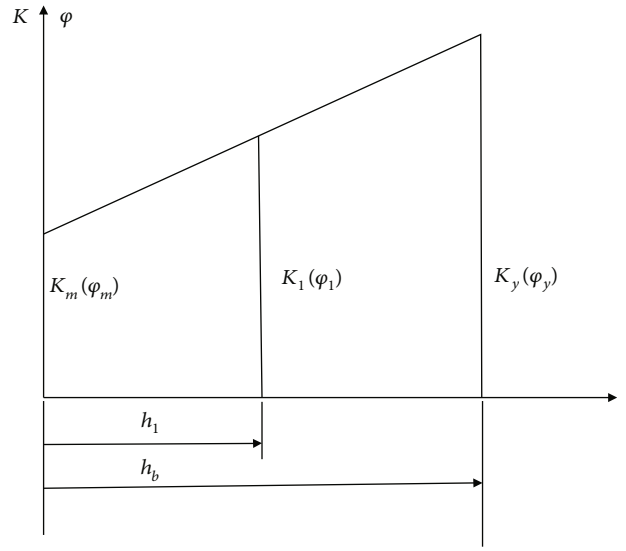

Figure 4: Parameter conversion relation of coal and rock mass.

According to the above,

$$a_r = \frac{2k_r \cos \varphi_r}{1\text{-}\sin \varphi_r}. \tag{14}$$

In this expression,

The value of k_r and $\cos \varphi_r/(1 - \sin \varphi_r)$ can be determined by referring to the ratio of a_1 and k_1 of $\cos \varphi_r/(1\text{-}\sin \varphi_r)$ in the x' direction, that is,

$$\frac{k_r}{\cos \varphi_r/(1 - \sin \varphi_r)} = \frac{k_1}{\cos \varphi_1/(1 - \sin \varphi_1)}. \tag{15}$$

Unite Equation (14) and Equation (15), we can get the expression of the internal friction angle and cohesion of the coal-rock mass in any direction in front of the working face:

$$\begin{cases} k_r = \sqrt{\dfrac{a_r k_1 (1 - \sin \varphi_1)}{2 \cos \varphi_1}}, \\ \varphi_r = \arcsin\left(\dfrac{a_r^2 - 4k_r^2}{a_r^2 + 4k_r^2}\right). \end{cases} \tag{16}$$

3.2. Mechanical Equation for the Parameter Change in the Plastic Zone of the Working Face of Crosscut Coal. Substituting Equation (16) into Equations (4), (5), and (6), we can get the expressions of stress distribution and width of plastic zone in the elastoplastic zone of crosscut coal:

$$\begin{cases} \sigma_r = \dfrac{1}{2}P_0(1+\lambda) - \dfrac{r_p^2 \sin \varphi_r}{2r^2}[P_0(1+\lambda) + 2K_r \mathrm{ctg}\varphi_r] - \dfrac{1}{2}P_0(1-\lambda)\left(1\text{-}4\dfrac{r_p^2}{r^2} + 3\dfrac{r_p^4}{r^4}\right)\cos 2\theta, \\ \sigma_\theta = \dfrac{1}{2}P_0(1+\lambda) + \dfrac{r_p^2 \sin \varphi_r}{2r^2}[P_0(1+\lambda) + 2K_r \mathrm{ctg}\varphi] + \dfrac{1}{2}P_0(1-\lambda)\left(1 + 3\dfrac{r_p^4}{r^4}\right)\cos 2\theta, \\ \tau_{r\theta} = \dfrac{1}{2}P_0(1-\lambda)\left(1 + 2\dfrac{r_p^2}{r^2} - 3\dfrac{r_p^4}{r^4}\right)\sin 2\theta, \end{cases} \tag{17}$$

$$R_p = R_0\left\{\frac{[P_0(1+\lambda) + 2\mathrm{K}_r \mathrm{ctg}\varphi_r](1 - \sin \varphi_r)}{2K_r \mathrm{ctg}\varphi_r}\right\}^{(1-\sin \varphi_r)/2 \sin \varphi_r} \cdot \left\{1 + \frac{(1 - \sin \varphi_r)P_0(1+\lambda)\cos 2\theta}{\sin \varphi_r[P_0(1+\lambda) + 2K_r \mathrm{ctg}\varphi_r]}\right\}, \tag{18}$$

$$\begin{cases} \sigma_{rp} = K_r \mathrm{ctg}\varphi_r\left[\left(\dfrac{r}{R_0}\right)^{2 \sin \varphi_r/(1-\sin \varphi_r)} - 1\right], \\ \sigma_{\theta p} = K_r \mathrm{ctg}\varphi_r\left[\dfrac{1 + \sin \varphi_r}{1 - \sin \varphi_r}\left(\dfrac{r}{R_0}\right)^{2 \sin \varphi_r/(1-\sin \varphi_r)} - 1\right]. \end{cases} \tag{19}$$

Equations (17), (18), and (19) are the analytical solutions for the stress distribution and the width of the plastic zone in front of the driving face.

4. Results and Analyses

The radius and distribution shape of the plastic zone in front of the driving face play an important role in the safety. It determined the degree of difficulty. Based on the stress state calculation model of crosscut coal mentioned before, combined with the actual engineering background and used Matlab numerical calculation software to carry out analysis of examples, the radius and distribution shape of the plastic zone in the whole process of crosscut coal and the effect of different overburden pressure of the plastic zone are analyzed. Then, use FLAC3D to simulate the overall process of crosscut coal. That provides the theoretical basis and design guidance for the drift construction in crosscut coal.

4.1. Shape Characteristics of Plastic Zone in Front of the Working Face in Crosscut Coal Process. According to the plastic zone equation of crosscut coal and its boundary conditions of the plastic zone, the width and distribution shape of the plastic zone in front of the working face at different distances from the coal seam are analyzed and calculated, respectively.

Assuming that the driving face is a hemisphere with a radius of 2 meters, the coal mass and rock mass in front of the working face are isotropic. Selecting a situation in which the coefficient of lateral pressure is 0.5, the inclination angle of the coal mass is 20 degrees, the internal friction angle of the coal is 20 degrees, the cohesion is 1.2 MPa, the internal friction angle of the rock mass is 35 degrees, the cohesion of it is 7 MPa, and the overburden pressure is 40 MPa (equivalent to buried depth of 1600 meters). And calculating the shape and width of the plastic zone in front of the working face, the normal distance between the driving face and the coal seam is 5 m, 4 m, 3 m, 2 m, and 1 m up to the uncovering coal point, respectively.

Figure 5 shows the distribution of coal-rock mass with different inclination angles at different vertical distances from the coal seam. Blue indicates the driving face, red line indicates the soft face, and black line indicates the strong face.

It can be seen from Figure 5 that there is an area where the radius of the plastic zone increases obviously at an angle

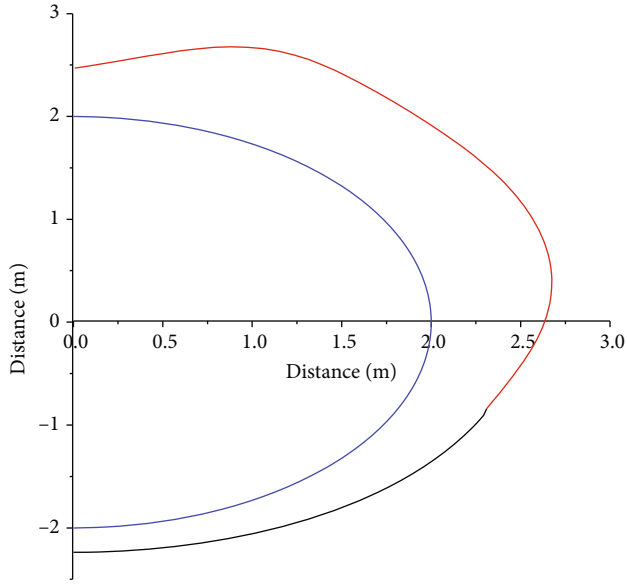

(a) Distribution of the plastic zone at 5 meters from the coal seam

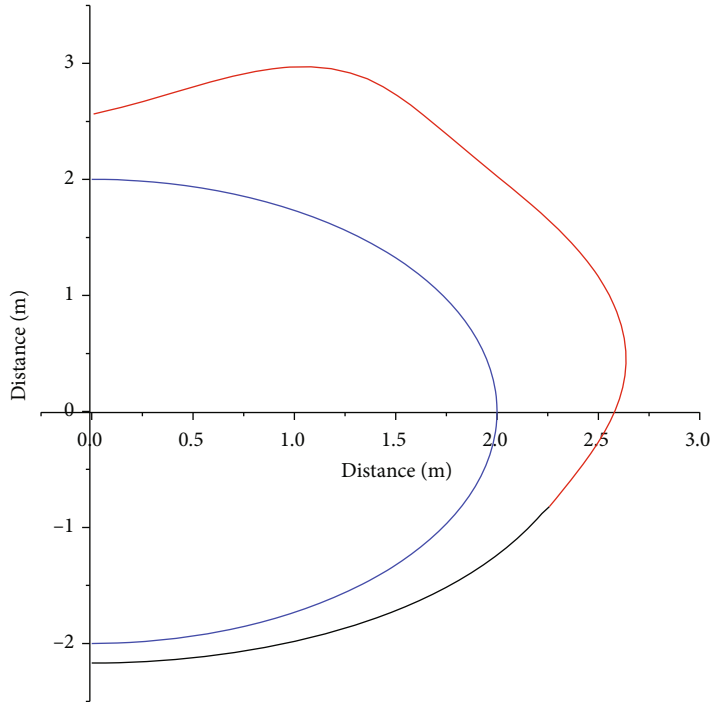

(b) Distribution of the plastic zone at 4 meters from the coal seam

Figure 5: Continued.

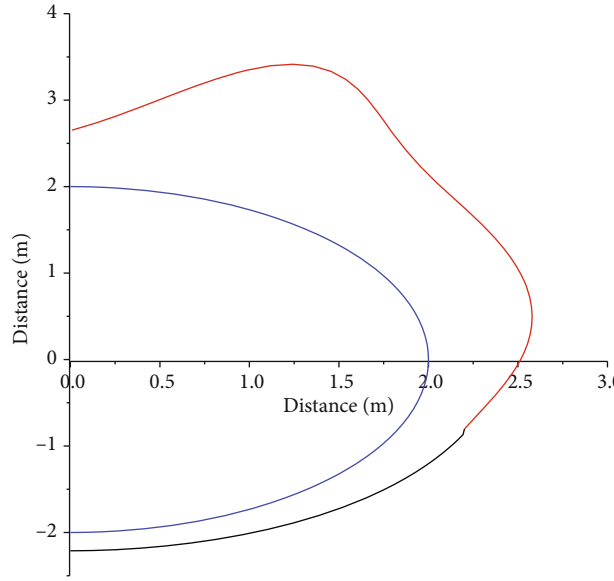

(c) Distribution of the plastic zone at 3 meters from the coal seam

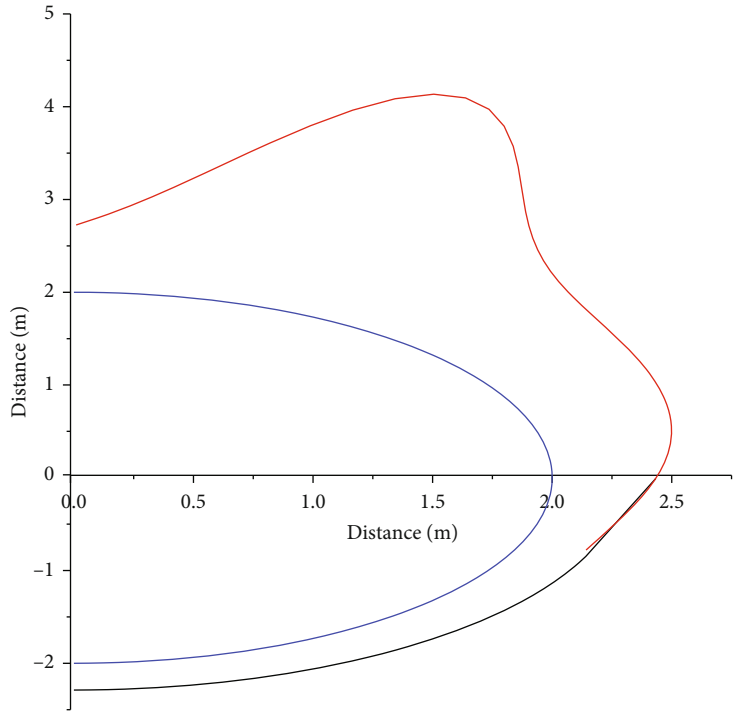

(d) Distribution of the plastic zone at 2 meters from the coal seam

Figure 5: Continued.

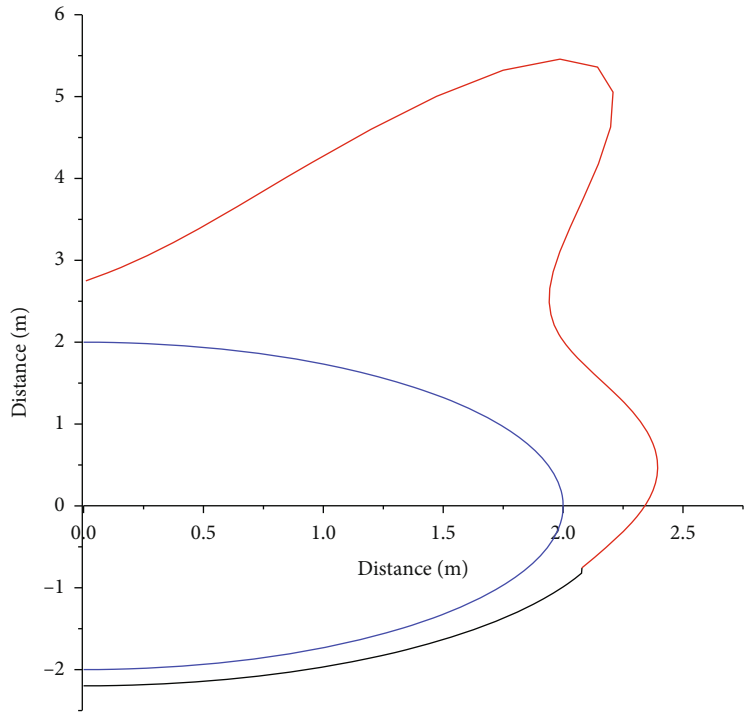

(e) Distribution of the plastic zone at 1 meters from the coal seam

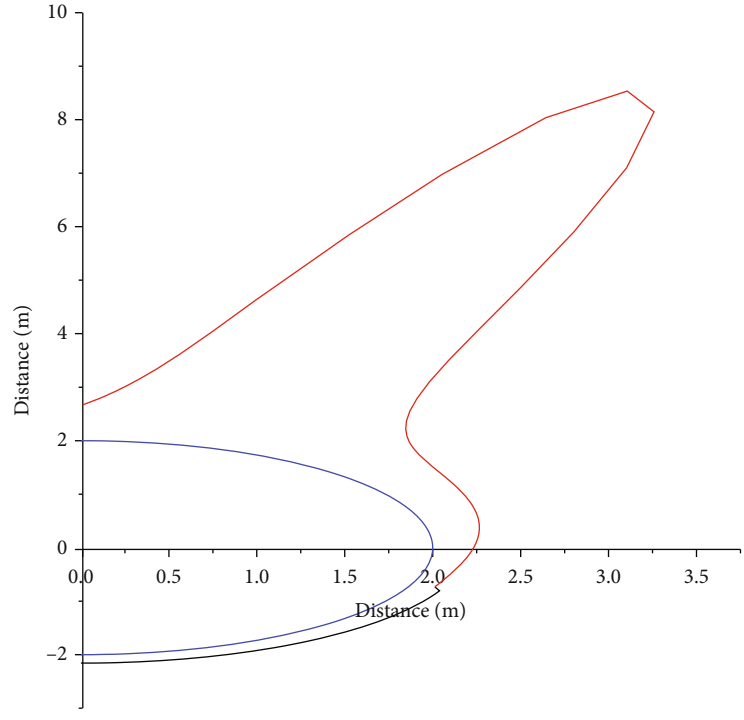

(f) Uncovering Coal point

Figure 5: Distribution shape of the plastic zone in crosscut coal process.

of 70 degrees from the driving direction. From Figures 5(a)–5(f), the change trend of the width and shape characteristics of the plastic zone during the process of crosscut coal can be seen. In the early stage of mining, the seam inclination has little effect on the width and shape distribution of the plastic zone in front of the working face, for the driving face is far away from the coal seam. As the driving face advances, the rock mass perpendicular to the coal mass thins gradually, the distance between the driving face and coal seam is getting shorter, the intensity of coal-rock mass decreases gradually as well, the stress concentration shifts from the rock mass to the coal mass, and the increment of the width of the plastic zone

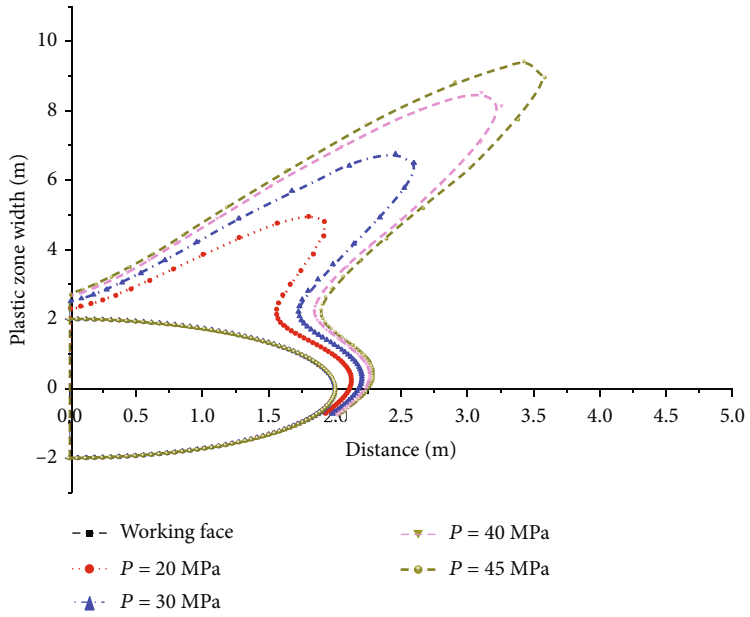

Figure 6: Morphological distribution of plastic zone at different tilt overburden pressure.

Table 1: Mechanical parameters of the model.

Stratum	Thickness	Internal friction angle (°)	Elasticity modulus (GPa)	Bulk modulus (GPa)	Shear modulus (GPa)	Tensile strength (MPa)	Cohesion	Density
Mudstone	12	26	2	11.8	3.9	1.7	3.7	2400
Sandy-mudstone	14	37	6	8.1	3.3	3	6.8	2400
Mudstone	3	26	2	11.8	3.9	1.7	3.7	2400
Coal	7	34	1	7	1.5	0.3	2.1	1410
Mudstone	3	26	2	11.8	3.9	1.7	3.7	2400
Sandy-mudstone	6	37	6	8.1	3.3	3	6.8	2400
Grained-sandstone	5	43	7	18.6	7.6	4	15.4	2600

perpendicular to the coal mass is more and more obvious, as the "semibutterfly" form in Figure 5 appears.

Comparing Figures 5(a)–5(f), it can be found that as the distance between the working face and the coal seam decreases constantly, the width of the plastic zone in the horizontal direction decreases from 0.6 meters to 0.3 meters. When uncovering the coal, the width of the plastic zone in the horizontal direction is 0.2 meters, and the width of the plastic zone in the vertical direction increases from 0.5 m to 0.85 m. When uncovering the coal, the width of the plastic zone in the vertical direction is 0.9 m, and the width of the plastic zone in the direction perpendicular to the coal seam increases from 0.85 m to 3.7 m. When uncovering the coal, the width of the plastic zone in this direction is 7 meters. Therefore, due to the existence of the coal seam, the width of the plastic zone in the horizontal and vertical directions varies but not much, while the width of the plastic zone in the direction perpendicular to the coal seam varies greatly. So, the shape distribution of the plastic zone changes from the initial "semielliptical" to "semibutterfly," especially obvious at coal uncovering point.

4.2. Distribution Shape and Width of the Plastic Zone at the Coal Uncovering Point under Different Overburden Pressure. With the mining depth increased, the problem of coal and gas outburst in crosscut coal becomes more and more serious. Therefore, this paper studies the shape and width of the plastic zone at the coal mining point under different overriding pressure. As show in Figure 6, the overriding pressure are 20 MPa, 30 MPa, 40 MPa, and 45 MPa.

From the width of plastic zone, when uncovering the coal, the width of plastic zone increases with the increase of overburden pressure. In the process, as the overburden pressure increased from 20 MPa to 45 MPa, the width of plastic zone in all directions increased, the radius of plastic zone in the driving (horizontal) direction increased from 2.1 m to 2.27 m, and the radius of plastic zone in the vertical direction of roadway increased from 2.31 m to 2.8 m. At the angle of 70

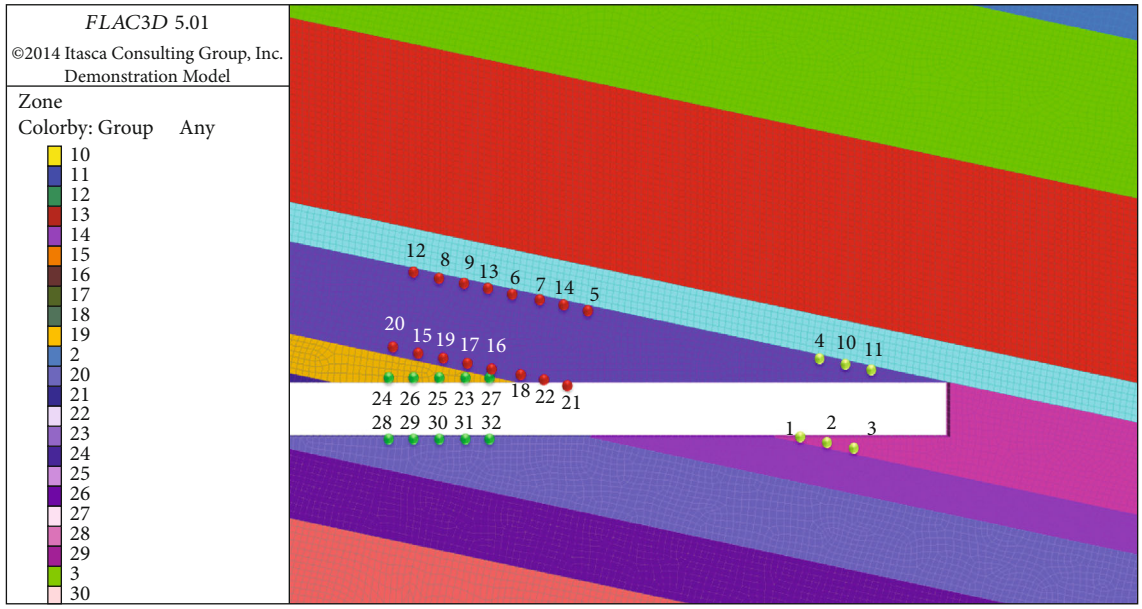

Figure 7: Schematic diagram of model monitoring points.

degrees, the radius of plastic zone is the largest, the increment of the width of plastic zone is the largest, and the radius of plastic zone increased from 5.27 m to 10.02 m. From the distribution shape of the plastic zone, with the increase of the overburden pressure, the deformation angle of the plastic zone is almost unchanged, but the width of the plastic zone is changed obviously, the "butterfly" of the plastic zone is more and more obvious. It indicates that the overburden pressure has a significant influence on the shape of the plastic zone of the coal-rock mass at the coal uncovering point, it also explains the phenomenon that with the increasing coal mining depth, nonoutburst mines begin to transform into outburst mines, and coal and gas outburst accidents become more and more serious.

4.3. FLAC3D Simulation Analysis of Crosscutting Coal. The FLAC3D is used to establish the model of gassy coal seam, and the gas pressure is 0.3 MPa. The geometric parameters of the model are set to be 200 m long, 50 m wide, and 100 m high, and the coal seam inclination is 12 degrees. Among them, the roadway is 5.5 m long, the straight wall is 1.5 m high, and the arch is 2.75 m. The mechanical parameters are shown in Table 1. And 32 monitoring points are arranged for this model (as shown in Table 1).

In order to visually analyze the dynamic changes of the plastic zone of the coal seam during the process from the rock seam to coal seam, the simulation results of the distribution of the plastic zone are shown in Figure 7, as the excavation distance reaches 16.5 m, 35 m, 51 m, 66 m, 69 m, 72 m, 76 m, 79.5 m, 82.5 m, 89.2 m, 95.9 m, 102.6 m, 109.3 m, and 116.52 m, and its coefficient of lateral pressure $\lambda = 0.6$.

According to Figure 8, it can be seen that the coal and rock seams are in a state of stress balance before excavation begins, and there is no stress failure area. When the excavation distance reaches 16.5 m, due to the short mining distance, the impact is minimal and almost no failure occurred. When the excavation distance reaches 35 m, in the middle of the roadway roof, due to the roof subsidence, a certain amount of tensile failure occurred. When the excavation distance reaches 51 m, the roof subsidence increased, and the tensile failure area increased; moreover, shear failure begins to occur in the upper coal seams at both ends of excavation. When the excavation distance reaches 66 m, the tensile failure area on the upper part of the roadway roof is almost unchanged, while the tensile failure area of the upper coal seam at both ends of the excavation is obviously increased, and the tensile failure force is superimposed. When the excavation distance reaches 76 m, the tensile failure area and shear failure area further increased, and the failure area is mainly concentrated in the first half of the coal seam above the roadway. When the excavation distance reaches 89.2 m, the second half of the coal seam above the roadway suffered more shear failure, and the failure area spread to the overlying rock seam of the coal seam. When the excavation distance reaches 89.2 m, the majority of the coal seam suffered tensile failure and shear failure, and the overlying rock seam also suffered a serious tensile failure. At this time, the coal and gas outburst is very likely to occur, so measures such as strengthening support and roof management must be taken to prevent such accidents and increase safety guarantee.

From the Flac3d simulation diagram, it can be seen that during the excavation process, the plastic zone first appeared in the upper left coal seam, and then appeared in the rock between the roadway and the coal seam. The plastic zone between coal and rock was connected together and gradually expanded. There is a little plastic zone in the lower part of the roadway that does not expand. It can be seen from the changes in the plastic zone that in the process of uncovering the coal in the crosscut, the expansion area of the plastic zone is basically on the side with the coal body. The "soft" feature of this side is very obvious, which is consistent with our "strong and weak surface" assumption.

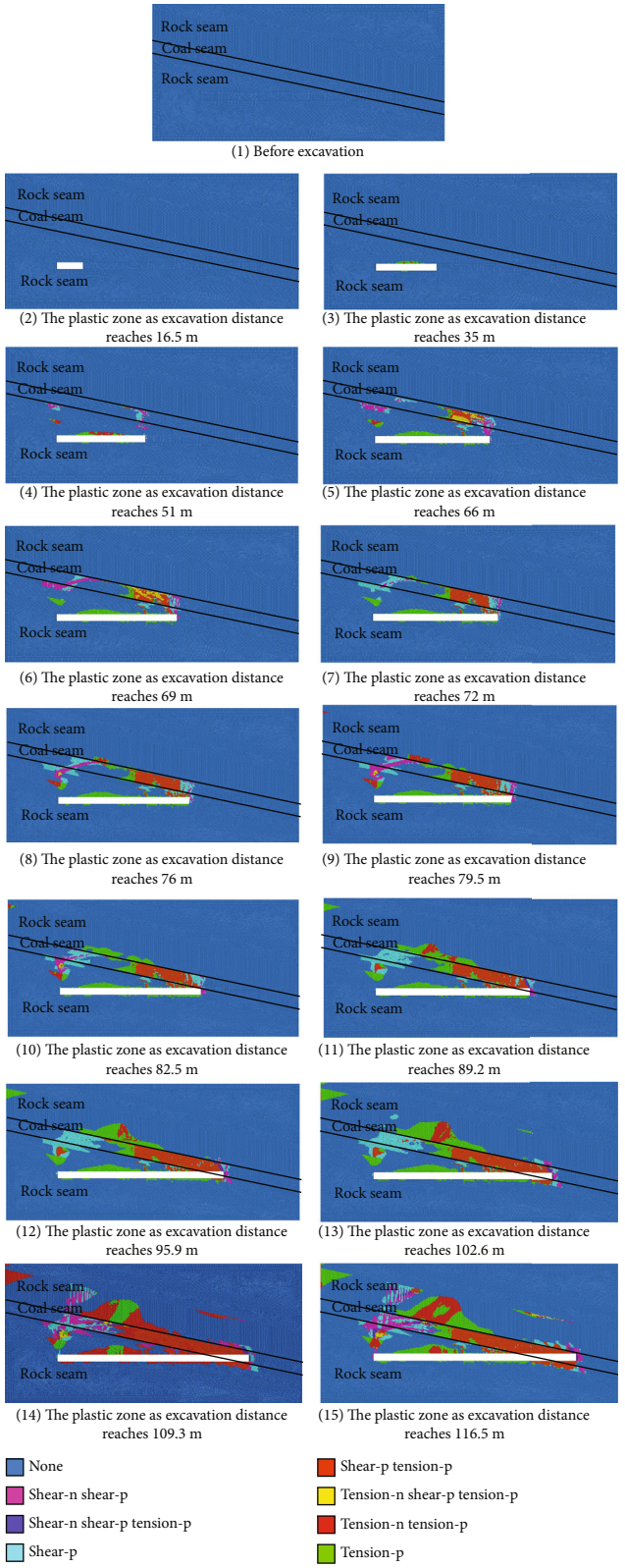

Figure 8: Distribution of plastic zone during excavation with coefficient of lateral pressure of 0.6.

5. Conclusion

With the increase of mining depth, coal and gas outburst accidents are becoming more and more serious. Taking the mechanism of outburst as the research object, this paper studies the stress state and distribution characteristics of plastic zone in the whole process from rock roadway driving to the end of uncovering coal by means of theoretical analysis and numerical simulation. The conclusions are as follows:

(1) The mechanical model of stress distribution and plastic zone width in front of semicircle arch roadway under nonuniform conditions was established, and analytic operation was carried out. The results suggest that the distribution of plastic zone in front of the rock roadway is "semidumbbell" before implementing crosscut coal. Through the analysis of examples, the morphological characteristics of the plastic zone in front of the roadway under different mechanical parameters are determined: the stress concentration effect of the rock roadway is obvious, the stress peak value is the highest, and the plastic zone range of the coal roadway is large

(2) Put forward the hypothesis of stress distribution on the "strong and soft face" of coal-rock mass in crosscut coal and studied the law of mechanical evolution in the roadway driving process. In this paper, it is believed that when the crosscut breaks through the coal seam, the distribution of the plastic zone in front of the roadway changes from "semidumbbell" to "semibutterfly." With the roadway advances, the width of the plastic zone becomes larger and larger. The width of the plastic zone in the horizontal and vertical directions varies but not much, while the width of the plastic zone in the direction perpendicular to the coal seam varies greatly. And the distribution of "semibutterfly" becomes more and more obvious. With the continuous increase of mining depth, the size of the plastic zone in the vertical direction of the coal seam in front of the working face has increased significantly, and the length of the two wings of the "butterfly" plastic zone has increased. From the form of the plastic zone, the maximum damage depth of the plastic zone in front of the working face is distributed on the side of the vertical coal seam

Data Availability

Data used in this article are available through email from the corresponding author.

Conflicts of Interest

The authors declare that there are no conflicts of interest.

References

[1] Britain, *Based on BP World Energy Prospect*, BP Energy Outlook, 2018, 2017 Edition.

[2] H. P. Kang, M. J. Fan, and F. Q. Gao, "Deformation and support of rock roadway at depth more than 1000 meters," *Chinese Journal of Rock Mechanics and Engineering*, vol. 34, no. 11, pp. 2161–2178, 2015.

[3] X. Wang, C. Liu, S. Chen, L. Chen, K. Li, and N. Liu, "Impact of coal sector's de-capacity policy on coal price," *Applied Energy*, vol. 265, article 114802, 2020.

[4] N. Victor, "A method for measuring coalbed methane content in coal strata without the loss of the gas," *Acta Geodynamica at Geomater*, vol. 15, no. 4, pp. 379–393, 2018.

[5] D. Changang, L. Sun, Y. Guo, G. Wang, and W. Cheng, "Experimental study on the coal damage characteristics of adsorption-instantaneous pressure relief in coal containing gases with different adsorption characteristics," *Applied Sciences-Basel*, vol. 9, no. 23, p. 5223, 2019.

[6] C. Wang, S. Yang, J. Li, X. Li, and C. Jiang, "Influence of coal moisture on initial gas desorption and gas-release energy characteristics," *Fuel*, vol. 232, no. 15, pp. 351–361, 2018.

[7] Z. Li, S. Liu, W. Ren, J. Fang, Q. Zhu, and Z. Dun, "Multiscale laboratory study and numerical analysis of water-weakening effect on shale," *Advances in Materials Science and Engineering*, vol. 2020, Article 5263431, 2020.

[8] Y. J. Chen, *Study on the Methods of Outburst Danger on Cross-cut Exposing Coal Prediction*, China University of Mining and Technology, Xuzhou, Jiangsu, 2015.

[9] Ministy of Land and Resources of the People's Republic of China, *China Mineral Resources Report*, 2017.

[10] Z. Li, H. Zhou, D. Hu, and C. Zhang, "Yield criterion for rock-like geomaterials based on strain energy and CMP model," *International Journal of Geomechanics*, vol. 20, no. 3, article 04020013, 2020.

[11] X. Zhang, Q. Wang, C Li, X. Sun, Z. Yan, and Y. Nie, "Numerical simulation of electrokinetic dissipation caused by elastic waves in reservoir rocks," *Geomechanics and Engineering*, vol. 19, no. 1, pp. 11–20, 2019.

[12] Q. Meng, H. Wang, M. Cai, W. Xu, X. Zhuang, and T. Rabczuk, "Three-dimensional mesoscale computational modeling of soil-rock mixtures with concave particles," *Engineering Geology*, vol. 277, Article 105802, 2020.

[13] X. G. Kong, E. Y. Wang, Q. L. Liu et al., "Dynamic permeability and porosity evolution of coal seam rich in CBM based on the flow-solid coupling theory," *Journal of Natural Gas Science & Engineering*, vol. 40, pp. 61–71, 2017.

[14] L. He, B. Lin, and H. Zhanbo, "Stress and displacement evolution features of opening seam in mine cross cut based on different in-situ rock stress and orientations," *Coal Science and Technology*, vol. 45, no. 10, pp. 88–95, 2017.

[15] Z. Zhiqiang, J. Junxiao, and J. Shen, "Promotion characteristics and induced outburst mechanisms of coal plastic zones in rock cross-cut coal uncovering," *Chinese Journal of Rock Mechanics and Engineering*, vol. 38, no. 2, pp. 343–352, 2019.

[16] H. Y. Pan, D. W. Yin, N. Jiang, and Z. G. Xia, "Crack initiation behaviors of granite specimens containing crossing-double-flaws with different lengths under uniaxial loading," *Advances in Civil Engineering*, vol. 2020, pp. 1–13.

[17] A. Zhou, K. Wang, L. Fan, and T. A. Kiryaeva, "Gas-solid coupling laws for deep high-gas coal seams," *Internation Journal of Mining Science and Technology*, vol. 27, no. 4, pp. 675–679, 2017.

[18] C. Wang, S. Yang, D. Yang, X. Li, and C. Jiang, "Experimental analysis of the intensity and evolution of coal and gas outbursts," *Fuel*, vol. 226, pp. 252–262, 2018.

[19] D. J. Black, "Review of coal and gas outburst in Australian underground coal mines," *International Journal of Mining Science and Technology*, vol. 29, no. 6, pp. 815–824, 2019.

[20] Z. Wang, Q. Hu, W. Guangcai, and S. Dongling, "Study on the distribution laws of mining pressure field and its control action on dynamic disasters in coal mines," *Journal of China Coal Society*, vol. 36, no. 4, pp. 623–627, 2011.

[21] D. Yanlu and Y. Z. Quentin, "An experimental investigation of the roles of water content and gas decompression rate for outburst in coal briquettes," *Fuel*, vol. 234, pp. 1221–1228, 2018.

[22] Y. Liang, F. Wang, Y. Luo, and Q. Hu, "Desorption characterization of methane and carbon dioxide in coal and its influence on outburst prediction," *Adsorption Science & Technology*, vol. 36, no. 7-8, pp. 1484–1495, 2018.

[23] W. D. Han and J. Shi, "Cross-hole exposing coal numerical simulation based on Yongshan mine," *Journal of Liaoning Technical University, Natural Science*, vol. 35, pp. 464–468, 2016.

[24] B. H. Yu, C. X. Su, and D. Wang, "Study of the features of outburst caused by rock cross-cut coal uncovering and the law of gas dilatation energy release," *International Journal of Mining ence and Technology*, vol. 25, no. 3, pp. 453–458, 2015.

[25] Z. Li, H. Liu, Z. Dun, L. Ren, and J. Fang, "Grouting effect on rock fracture using shear and seepage assessment," *Construction and Building Materials*, vol. 242, Article 118131, 2020.

[26] W. A. Griffith, J. Becker, K. Cione, T. Miller, and E. Pan, "3D topographic stress perturbations and implications for ground control in underground coal mines," *International Journal of Rock Mechanics and Mining Sciences*, vol. 70, pp. 59–68, 2014.

[27] C. Jiang, M. Duan, G. Yin et al., "Experimental study on seepage properties, AE characteristics and energy dissipation of coal under tiered cyclic loading," *Engineering Geology*, vol. 221, pp. 114–123, 2017.

[28] J. Li, Q. Hu, M. Yu, X. Li, J. Hu, and H. Yang, "Acoustic emission monitoring technology for coal and gas outburst," *Energy Science and Engineering*, vol. 7, no. 2, pp. 443–456, 2019.

[29] K. Gao, Z. G. Liu, and J. Liu, "Effect of geostress on coal and gas outburst in the uncovering tectonic soft coal by cross-cut," *Chinese Journal of Rock Mechanics & Engineering*, vol. 34, no. 2, pp. 305–312, 2015.

[30] C. A. Tang and H. Y. Liu, "Numerical approach on outburst in crosscutting in coal seam containing gas," *Chinese Journal of Rock Mechanics & Engineering*, vol. 10, pp. 1467–1472, 2002.

[31] J. P. Zuo, H. P. Xie, A. M. Wu, and J. F. Liu, "Investigation on failure mechanisms and mechanical behaviors of deep coal-rock single body and combined body," *Chinese Journal of Rock Mechanics and Engineering*, vol. 30, no. 1, pp. 84–92, 2011.

[32] N. Ma, L. Ji, and Z. Zhiqiang, "Distribution of the deviatoric stress field and plastic zone in circular roadway surrounding rock," *Journal of China University of Mining and Technology*, vol. 44, no. 2, pp. 206–213, 2015.